Two-Channel Partially Coupled Exclusion Process With Mutually Interactive Langmuir Kinetics

Traffic and Granular Flow Conference (TGF 2015),
TU Delft

Arvind Kumar Gupta

Indian Institute of Technology Ropar
Rupnagar, Punjab - 140001, India.

Outline

- Motivation
- Basic definitions
- Two-lane TASEP with mutually interactive LK Model
- Results
- Conclusions
- References

Motivation

- Molecular motors are motor proteins which consume chemical energy and move along polymer filaments of the cytoskeleton, which act as macromolecular highways.
- By understanding the intracellular transport carried out by motor proteins, one can get insight about certain diseases like left-right body determination and tumor suppression etc.
- In the past decades, motion of motor proteins has been studied by mimicking it using totally asymmetric simple exclusion process (TASEP) models.
- The study of TASEP has contributed to a large extent in understanding the physics of many non-equilibrium phenomena such as vehicular flow in traffic, translation of mRNA and protein synthesis etc.

Motivation (contd...)

Why study TASEP?

TASEP provides a good description of vehicular traffic, the kinetics of bio-polymerization, polymer dynamics in dense media, diffusion through membrane channels, dynamics of motor proteins moving along rigid filaments, etc.

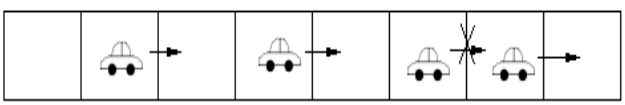

Figure 1 : Vehicles moving on road

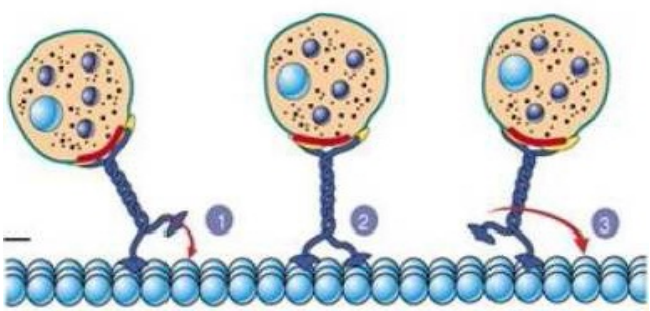

Figure 2 : Molecular motors moving on Filament

Totally Asymmetric Simple Exclusion Process (TASEP)

Definition

The TASEP is a Markov process, consisting of particles located on a discrete lattice that evolves in continuous time. It describes the totally biased diffusion of particles on a one-dimensional lattice in a preferred direction. In TASEP-

- Particle-particle interactions are ignored.
- Particles follow hard-core exclusion principle.

TASEP with open boundaries: Dynamical Rules

- A particle can enter the lattice with a rate α provided entrance site is empty.
- A particle can leave the lattice with a rate β provided exit site is occupied.
- In the bulk, particle can move to its neighbouring site with unit rate iff target site is vacant.

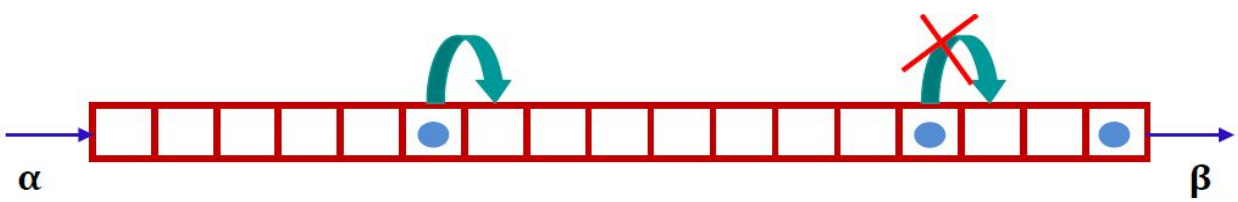

Figure 3 : TASEP on a one-dimensional lattice with finite length. Crossed arrow show that particles obey hard-core exclusion principle.

Langmuir Kinetics

Definition

It is the process by which particles can attach to the bulk lattice sites as well as detach from the bulk lattice sites. This attachment-detachment dynamics occur at certain rates, denoted by w_a and w_d, respectively.

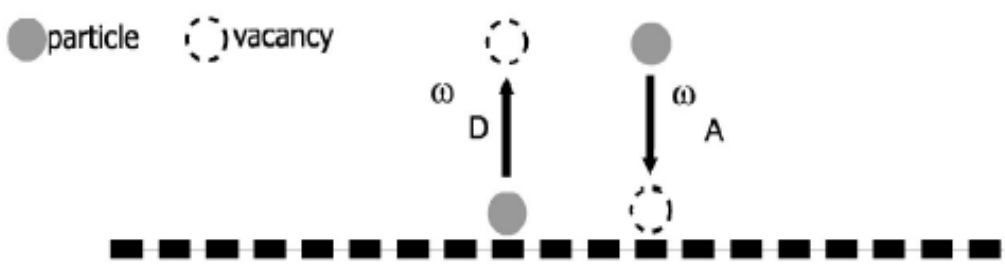

Figure 4 : Illustration of Langmuir Kinetics

Asymmetric coupling in Two-lane TASEP with mutually interactive LK Model

Two-lane TASEP with mutually interactive LK

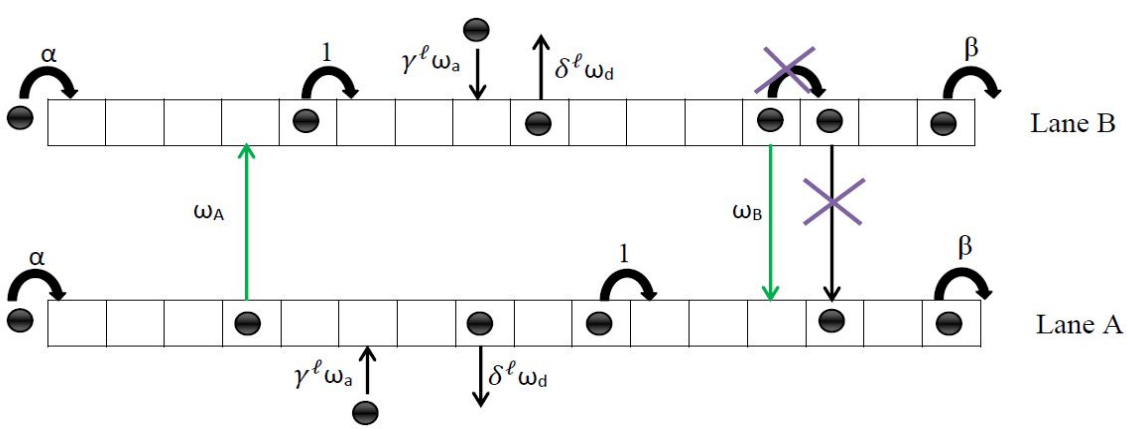

Figure 5 : Schematic diagram of the model

mutually interactive LK dynamics

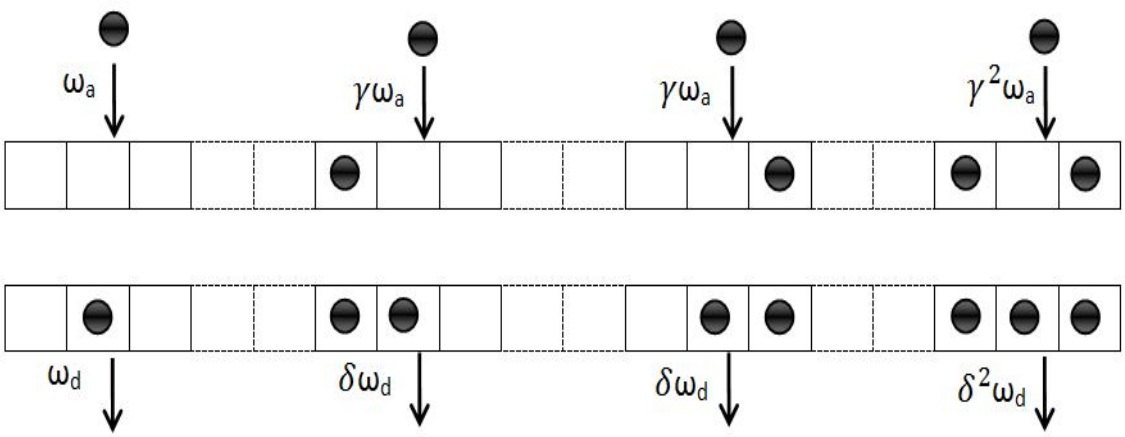

Figure 6 : Schematic diagram of MILK

Master equation: Flow of probability in configurational space

The probability of finding the system in configuration C at time t is denoted by $P_C(t)$. The time evolution of $P_C(t)$ is described by the master equation:

$$\frac{dP_C(t)}{dt} = \underbrace{\sum_{C'} W_{CC'} P_{C'}(t)}_{\text{Gain term}} - \underbrace{\sum_{C} W_{C'C} P_C(t)}_{\text{Loss term}}$$

where $W_{CC'}$ is the rate of transition (probability per unit time) from configuration C to C' ; C and C' differ by one particle hop.

Two-lane TASEP with mutually interactive LK (contd....)

Bulk density time evolution

$$
\begin{aligned}
\frac{d\langle\tau_{i,j}\rangle}{dt} =& \langle\tau_{i-1,j}(1-\tau_{i,j})\rangle - \langle\tau_{i,j}(1-\tau_{i+1,j})\rangle \\
&+ \omega_a\langle(1-\tau_{i-1,j})(1-\tau_{i,j})(1-\tau_{i+1,j})\rangle \\
&+ \gamma\omega_a\langle(1-\tau_{i,j})[(1-\tau_{i+1,j})\tau_{i-1,j} + (1-\tau_{i-1,j})\tau_{i+1,j}]\rangle \\
&+ \gamma^2\omega_a\langle\tau_{i-1,j}(1-\tau_{i,j})\tau_{i+1,j}\rangle \\
&- \omega_d\langle\tau_{i,j}(1-\tau_{i-1,j})(1-\tau_{i+1,j})\rangle \\
&- \delta\omega_d\langle\tau_{i,j}((1-\tau_{i-1,j})\tau_{i+1,j} + (1-\tau_{i+1,j})\tau_{i-1,j})\rangle \\
&- \delta^2\omega_d\langle\tau_{i-1,j}\tau_{i,j}\tau_{i+1,j}\rangle \\
&\mp \omega_A\langle\tau_{i,A}\tau_{i+1,A}(1-\tau_{i,B})\rangle \pm \omega_B\langle\tau_{i,B}\tau_{i+1,B}(1-\tau_{i,A})\rangle.
\end{aligned}
$$

Two-lane TASEP with mutually interactive LK (contd....)

Boundary density time evolution (contd....)

$$\frac{d\langle\tau_{1,j}\rangle}{dt} = \alpha\langle(1-\tau_{1,j})\rangle - \langle\tau_{1,j}(1-\tau_{2,j})\rangle,$$
$$\frac{d\langle\tau_{N,j}\rangle}{dt} = \langle\tau_{N-1,j}(1-\tau_{N,j})\rangle - \beta\langle\tau_{N,j}\rangle.$$

Where, $\langle ... \rangle$ denotes statistical average and $\tau_j^i (j = A, B; i = 2, 3, ..., N-1)$ denote the binary occupation numbers with values 1 and 0 according to the site is occupied or empty, respectively.

Mean-field Analysis

In order to solve master equations of proposed model, we ignore particle-particle correlations and factorize the correlations using mean-field approximation which gives

$$\langle \tau_{i,j}\tau_{i+1,j}\rangle = \langle \tau_{i,j}\rangle\langle \tau_{i+1,j}\rangle$$

Two-lane TASEP with mutually interactive LK (contd....)

Continuum limit of the model

Define $\epsilon = 1/N$, $t' = t/N$, $\omega_a = \Omega_a/N, \omega_d = \Omega_d/L, \omega_A = \Omega_A/N, \omega_B = \Omega_B/N$ and write $\langle \tau_j^i \rangle = \rho_j^i$, we get

$$\frac{\partial}{\partial t'}\begin{bmatrix}\rho_A\\ \rho_B\end{bmatrix} + \frac{\partial}{\partial x}\begin{bmatrix}-\frac{\epsilon}{2}\frac{\partial \rho_A}{\partial x} + \rho_A(1-\rho_A)\\ -\frac{\epsilon}{2}\frac{\partial \rho_B}{\partial x} + \rho_B(1-\rho_B)\end{bmatrix} = S, \tag{1}$$

where

$$S = \begin{bmatrix}\Omega_a(1-\rho_A)(1+\rho_A(\delta-1))^2 - \Omega_d\rho_A(1+\rho_A(\gamma-1))^2 \\ -\Omega_A\rho_A^2(1-\rho_B) + \Omega_B\rho_B^2(1-\rho_A) \\ \Omega_a(1-\rho_B)(1+\rho_B(\delta-1))^2 - \Omega_d\rho_B(1+\rho_B(\gamma-1))^2 \\ +\Omega_A\rho_A^2(1-\rho_B) - \Omega_B\rho_B^2(1-\rho_A)\end{bmatrix}.$$

Two-lane TASEP with mutually interactive LK (contd....)

Steady-state equations

$$\frac{\epsilon}{2}\frac{d^2\rho_A}{dx^2} + (2\rho_A - 1)\frac{d\rho_A}{dx} + \Omega_a(1-\rho_A)(1+\rho_A(\delta-1))^2$$
$$-\Omega_d\rho_A(1+\rho_A(\gamma-1))^2 - \Omega_A\rho_A^2(1-\rho_B) + \Omega_B\rho_B^2(1-\rho_A) = 0,$$
$$\frac{\epsilon}{2}\frac{d^2\rho_B}{dx^2} + (2\rho_B - 1)\frac{d\rho_B}{dx} + \Omega_a(1-\rho_B)(1+\rho_B(\delta-1))^2$$
$$-\Omega_d\rho_B(1+\rho_B(\gamma-1))^2 + \Omega_A\rho_A^2(1-\rho_B) - \Omega_B\rho_B^2(1-\rho_A) = 0.$$

Boundary conditions

$\rho_A(0) = \rho_B(0) = \alpha,\ \rho_A(1) = \rho_B(1) = 1 - \beta = \gamma.$

Steady-state solution: Boundary Layer Analysis

- To find the steady-state solution of the coupled non-linear system, we employ singular perturbation technique.
- The main idea of boundary layer analysis is to compute the outer solution and inner solution.
- Outer solution- The bulk part of the solution that is found in limit of $\epsilon \longrightarrow 0$ is called outer solution.
- Inner solution- The boundary layer solution that is obtained by eliminating source and sink terms is called inner solution.

Boundary layer analysis

Outer Solution: The solution of

$$(2\rho_A - 1)\frac{d\rho_A}{dx} + \Omega_a(1-\rho_A)(1+\rho_A(\delta-1))^2$$
$$-\Omega_d\rho_A(1+\rho_A(\gamma-1))^2 - \Omega_A\rho_A^2(1-\rho_B) + \Omega_B\rho_B^2(1-\rho_A) = 0,$$
$$(2\rho_B - 1)\frac{d\rho_B}{dx} + \Omega_a(1-\rho_B)(1+\rho_B(\delta-1))^2$$
$$-\Omega_d\rho_B(1+\rho_B(\gamma-1))^2 + \Omega_A\rho_A^2(1-\rho_B) - \Omega_B\rho_B^2(1-\rho_A) = 0.$$

is called Outer solution or bulk solution. It has been computed numerically.

Boundary layer analysis (Contd...)

Inner Solution: The solution of

$$\frac{\epsilon}{2}\frac{d^2\rho_A}{dx^2} + (2\rho_A - 1)\frac{d\rho_A}{dx} = 0$$
$$\frac{\epsilon}{2}\frac{d^2\rho_B}{dx^2} + (2\rho_B - 1)\frac{d\rho_B}{dx} = 0.$$

is called Inner solution or boundary layer solution.
Define $\widetilde{x} = \frac{x - x_d}{\epsilon}$; where x_d is the position of the boundary layer.
We need to solve

$$\frac{d\rho_{j,in}}{d\widetilde{x}} = 2(a_j + \rho_{j,in} - \rho_{j,in}^2)$$

Here, a_j is computed from the matching condition.

Boundary layer analysis (Contd...)

Suppose, boundary layer appears at right boundary ($x = 1$) in lane-j, the matching condition requires

$$\rho_{j,in}(\widetilde{x} \to -\infty) = \rho_{j,out}(x = 1) = \rho_{j,o}.$$

Here, $\rho_{j,o}$ is value of left outer solution in lane-j at $x = 1$. Putting $a_j = \rho_{j,o}^2 - \rho_{j,o}$, we get

$$\rho_{j,in} = \frac{1}{2} + \frac{|2\rho_{j,o} - 1|}{2} \tanh\left(\frac{\widetilde{x}}{w_j} + \xi_j\right),$$

where $w_j = \frac{1}{|2\rho_{j,o}-1|}$ and $\xi_j = \tanh^{-1}\left(\frac{2\gamma-1}{|2\rho_{j,o}-1|}\right)$

Within LD as well as HD phase, the slope of boundary layer is negative for $\gamma < \rho_{j,o}(\alpha)$ and the inner solution in this region is

$$\rho_{j,in} = \frac{1}{2} + \frac{|2\rho_{j,o} - 1|}{2} \coth\left(\frac{\widetilde{x}}{w_j} + \hat{\xi}_j\right),$$

where $\hat{\xi}_j = \coth^{-1}\left(\frac{2\gamma - 1}{|2\rho_{j,o} - 1|}\right)$.

Results

- The results are divided into two parts based on the symmetric or antisymmetric LK rates.
- In the symmetric case, attachment and detachment rates are modified in a similar fashion while in the antisymmetric case, if attachment rate is enhanced than the detachment rate is reduced by the same amount and vice-versa.

Symmetric LK rates

- To investigate the effect of mutual interactions with symmetric modified LK, we choose $\gamma = \delta = 1 + \theta$, where $\theta \geq -1$. Here, θ represents the strength of the mutual interaction under symmetric LK rates.

Symmetric LK rates

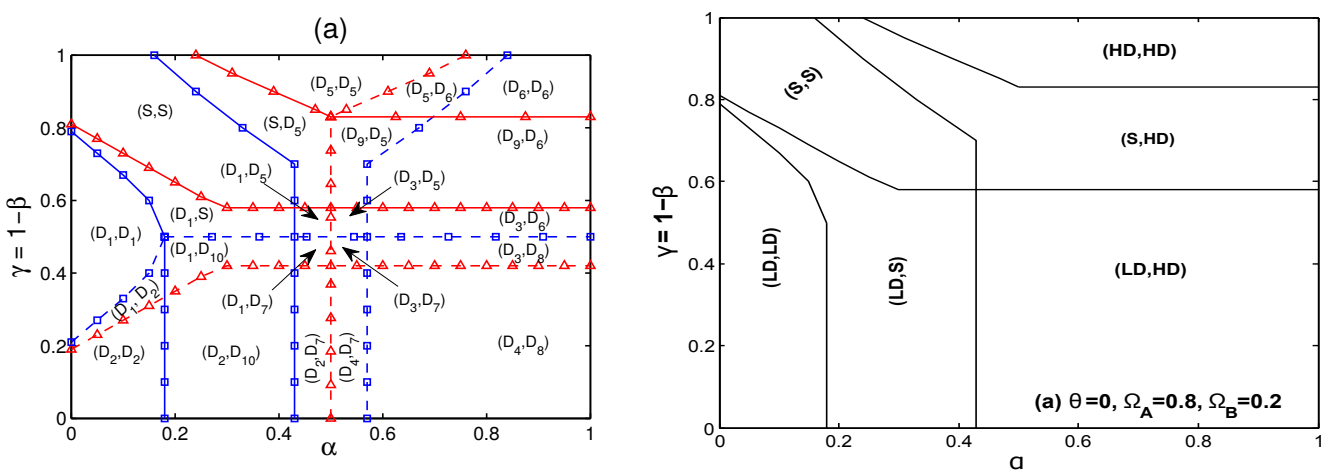

Figure 7 : Phase diagram for $\theta = 0$, $\Omega_d = 0.2$, $\Omega_A = 0.8$, and $\Omega_B = 0.2$. Solid and dashed curves denote bulk and surface transitions, respectively. (b) Classification of phases on the basis of bulk transitions only.

Notations

The following notations are used:

- D_1, tanh-r; D_2, coth-r; D_3, tanh-r with a LBL; D_4, coth-r with a LBL; D_5, tanh-l; D_6, coth-l; D_7, tanh-l with a RBL; D_8, coth-l with a RBL; D_9, S plus a LBL; and D_{10}, S plus a RBL.
- Here S denotes shock and LBL and RBL denote the left boundary layer and right boundary layer, respectively.
- Curves marked with triangles and squares represent phase boundaries of lanes A and B, respectively. Solid and dashed curves denote bulk and surface transitions, respectively.

Effect of θ

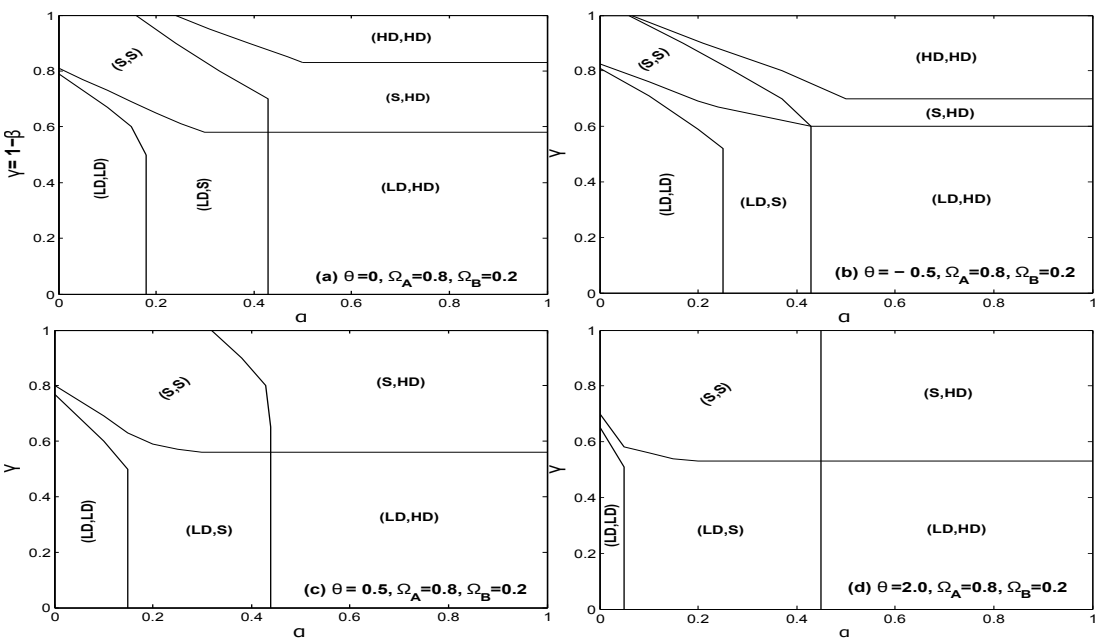

Figure 8 : Phase diagrams for various values of θ with $\Omega_a = \Omega_d = 0.2$, $\Omega_A = 0.8$ and $\Omega_B = 0.2$.

Monte-Carlo Simulation Results

- Theoretical results of continuum mean field equations are validated by Monte Carlo simulations using random sequential update rules for system size N = 1000.
- Simulations are carried out for 10^{10} time steps and first 5% are discarded to ensure the occurrence of stationary state.
- To compute average densities in both lanes time averages over an interval of 10N are taken.

Density Profiles for symmetric LK rates for $\theta = 2$

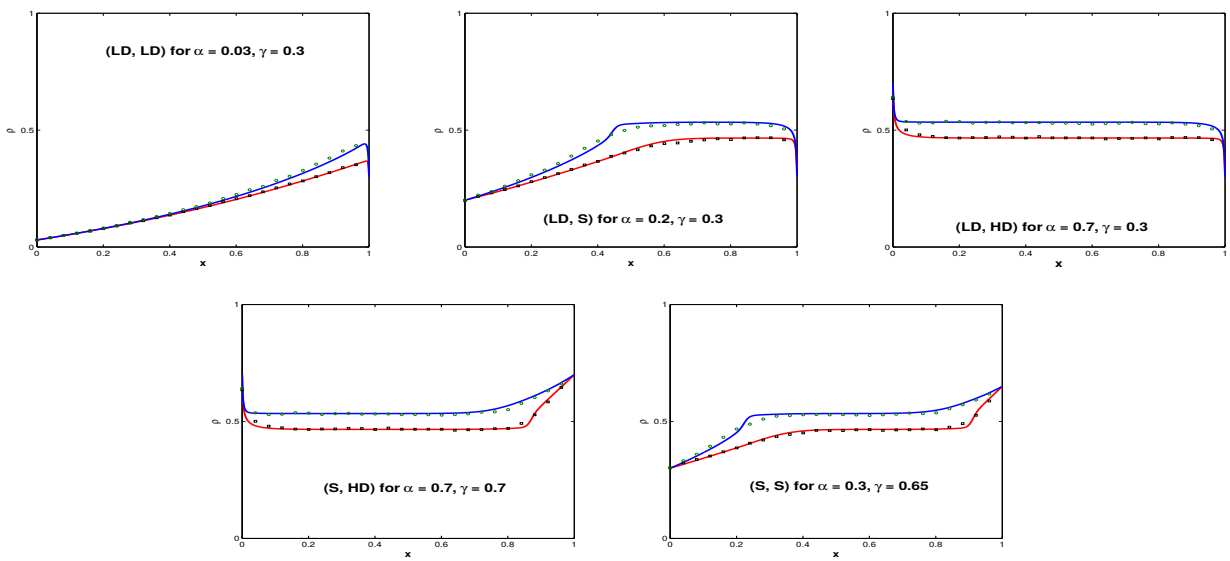

Figure 9 : Density profiles in various phases for $\theta = 2$, $\Omega_a = \Omega_d = 0.2$, $\Omega_A = 0.8$ and $\Omega_B = 0.2$

Effect of enhanced LK rates on phase diagram

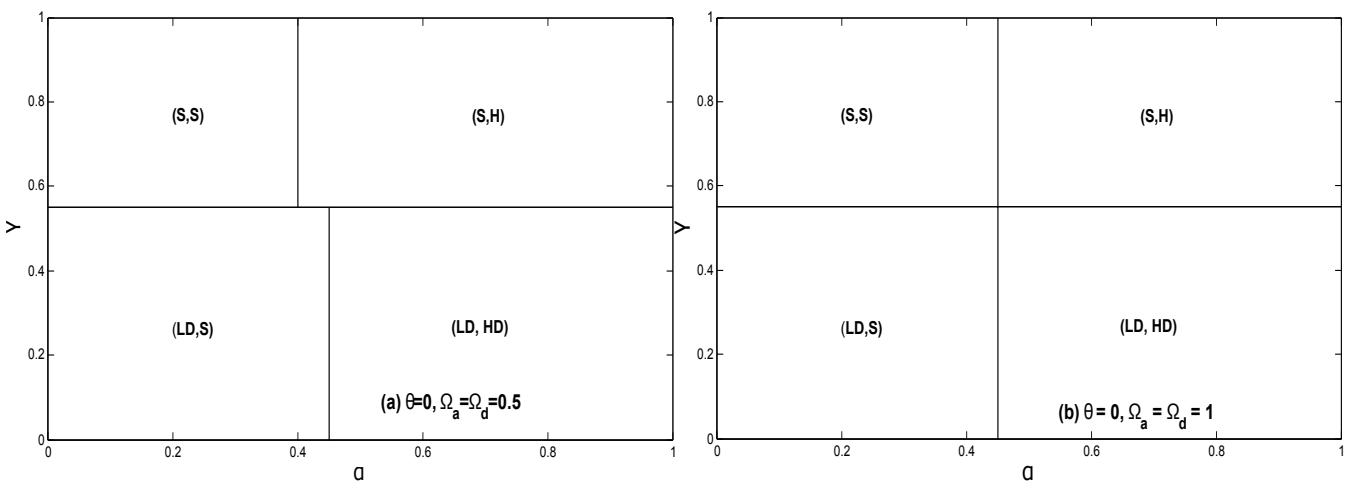

Figure 10 : Phase diagrams for (a) $\Omega_a = \Omega_d = 0.5$ (b) $\Omega_a = \Omega_b = 1$ with $\theta = 0$, $\Omega_A = 0.8$ and $\Omega_B = 0.2$.

Mutual interaction with antisymmetric LK rates

- To investigate the effect of mutual interactions with antisymmetric modified LK, we choose $\gamma = 1 + \phi, \delta = 1 - \phi$. Here, ϕ is a constant having the range [-1,1].

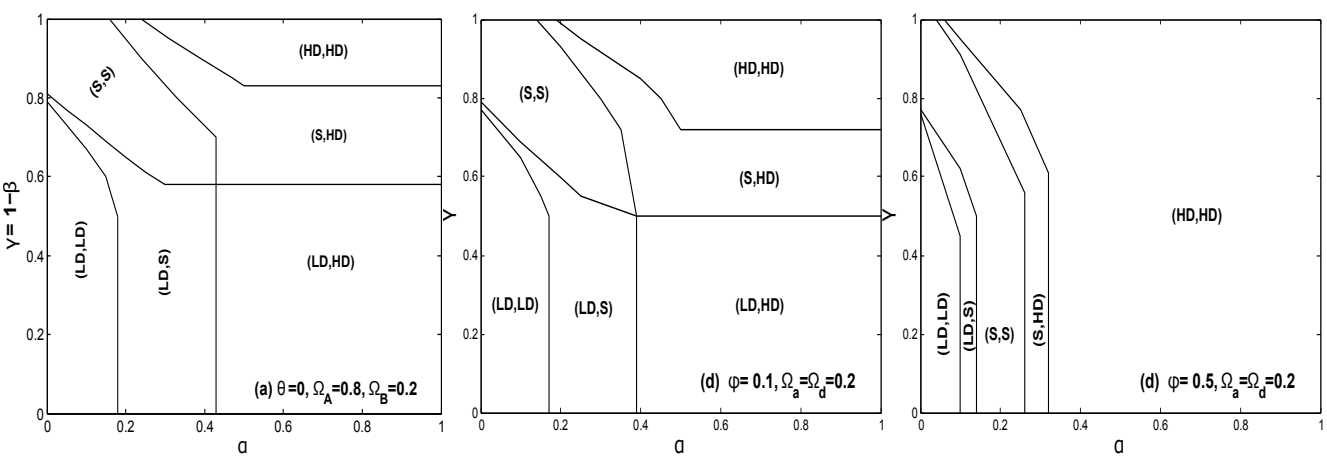

Figure 11 : Phase diagrams for (a) $\phi = 0$ (b) $\phi = 0.1$ (c) $\phi = 0.5$ with $\Omega_a = \Omega_d = 0.2$, $\Omega_A = 0.8$ and $\Omega_B = 0.2$.

Density Profiles for antisymmetric LK rates with $\phi = 0.5$

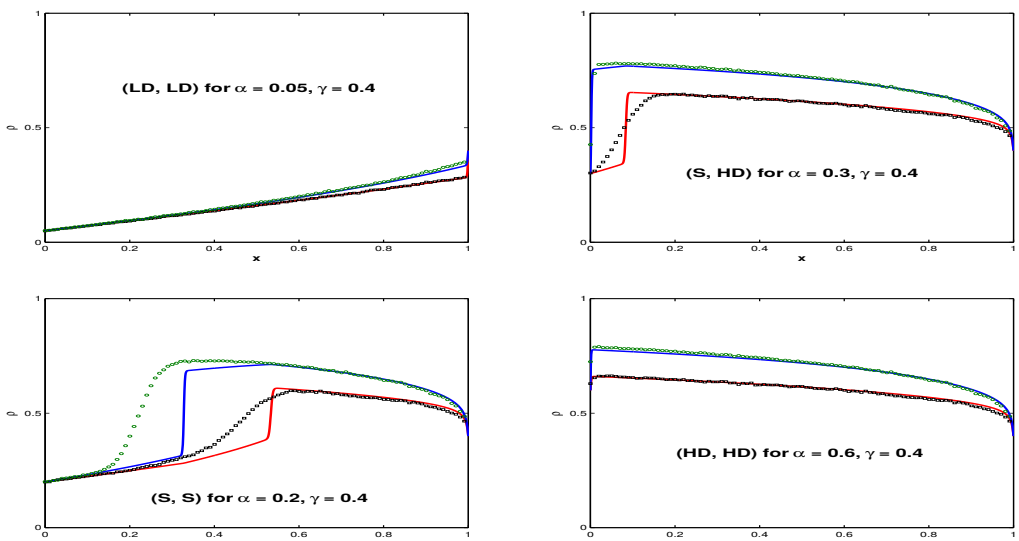

Figure 12 : Density profiles in various phases for $\phi = 0.5$, $\Omega_a = \Omega_d = 0.2$ and $\Omega_A = 0.8$ and $\Omega_B = 0.2$.

Effect of negative ϕ

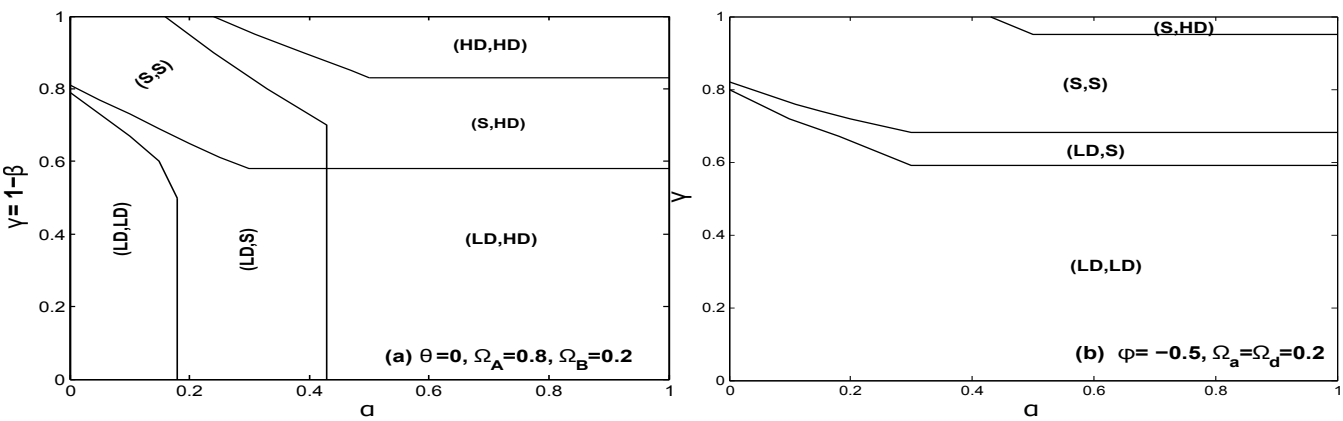

Figure 13 : Phase diagrams for (a) $\phi = 0$ (b) $\phi = -0.5$ with $\Omega_a = \Omega_d = 0.2$, $\Omega_A = 0.8$ and Ω_B=0.2.

Effect of negative ϕ(Contd...)

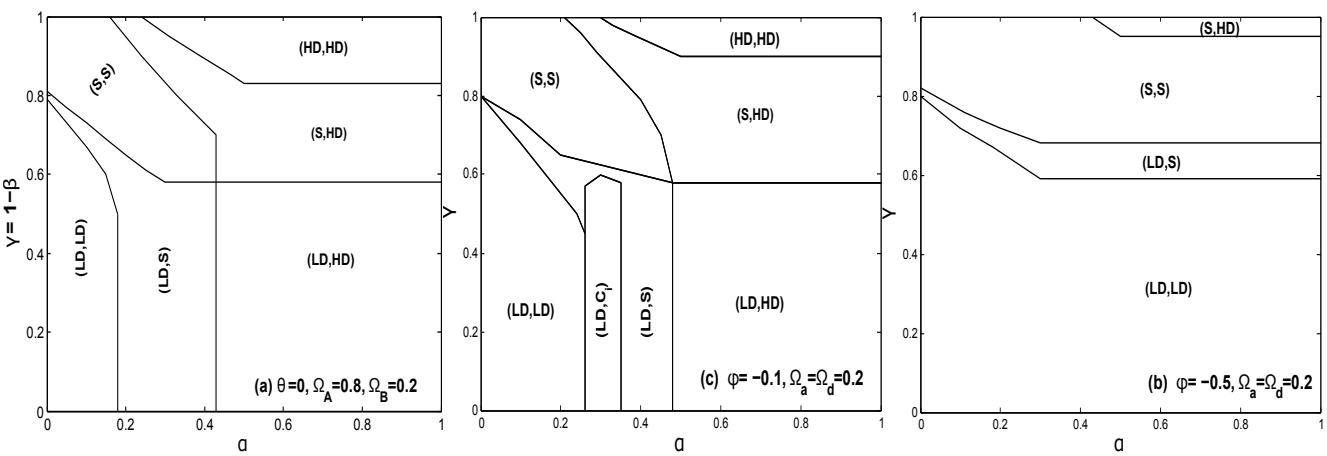

Figure 14 : Phase diagrams for (a) $\phi = 0$ (b) $\phi = -0.1$ (c) $\phi = -0.5$ with $\Omega_a = \Omega_d = 0.2$, $\Omega_A = 0.8$ and $\Omega_B = 0.2$.

Density Profiles for antisymmetric LK rates with $\phi = -0.5$

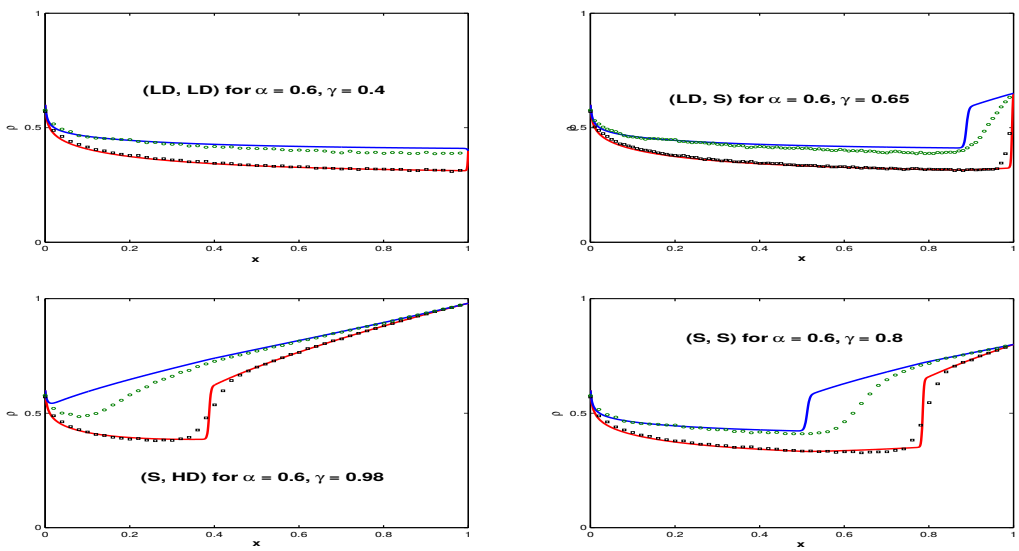

Figure 15 : Density profiles in various phases for $\phi = -0.5$, $\Omega_a = \Omega_d = 0.2$ and $\Omega_A = 0.8$ and $\Omega_B = 0.2$.

Conclusions

- We have studied a two-channel asymmetrically coupled TASEP with mutually interactive LK using mean-field analysis along with singular perturbation technique.
- The effect of mutual interactions on the phase diagram for two different situations of attachment and detachment (LK) rates is analyzed.
- We have noticed that mean-field theory breaks down in the neighborhood of shock position in lane-B for antisymmetric LK rates due to neglected correlations.

References

- E. Frey, A. Parmeggiani, and T. Franosch, Genome Informatics 15, 46 (2004).
- J. Krug, Physical review letters 67, 1882 (1991).
- A. Parmeggiani, T. Franosch, and E. Frey, Physical review letters 90, 086601 (2003).
- J. Howard, Mechanics of motor proteins and the cy- toskeleton (Sinauer Associates; Sunderland, MA, 2001).
- A. Parmeggiani, T. Franosch, and E. Frey, Physical Review E 70, 046101 (2004).
- A. Vilfan, E. Frey, F. Schwabl, M. Thormahlen, Y.-H. Song, and E. Mandelkow, Journal of molecular biology 312, 1011 (2001).
- H. D. Vuijk, R. Rens, M. Vahabi, F. C. MacKintosh, and A. Sharma, Physical Review E 91, 032143 (2015).

References

- W. H. Roos, O. Camp'as, F. Montel, G. Woehlke, J. P. Spatz, P. Bassereau, and G. Cappello, Physical biology 5, 046004 (2008).
- D. Celis-Garza, H. Teimouri, and A. B. Kolomeisky, Journal of Statistical Mechanics: Theory and Experiment 2015, P04013 (2015).
- A. K. Gupta and I. Dhiman, Physical Review E 89, 022131 (2014).
- I. Dhiman and A. K. Gupta, Physical Review E 90, 012114 (2014).

Acknowledgements

I would like to acknowledge IIT Ropar for providing facilities and Department of Science and Technology(DST), Government of India for providing financial support.

Thank You